

# The effects of ZnO particles on the color homogeneity of phosphor-converted high-power white led light sources

Nguyen Thi Phuong Loan<sup>1</sup>, Nguyen Doan Quoc Anh<sup>2</sup>

<sup>1</sup>Faculty of Fundamental 2, Posts and Telecommunications Institute of Technology, Vietnam

<sup>2</sup>Power System Optimization Research Group, Faculty of Electrical and Electronics Engineering, Ton Duc Thang University, Vietnam

---

## Article Info

### Article history:

Received Sep 26, 2019

Revised Apr 22, 2020

Accepted May 4, 2020

### Keywords:

Color rendering index

Lambert-Beer law

Luminous efficacy

White LED

---

## ABSTRACT

Color homogeneity is one of the goals to continuously improve WLED. Among the methods for enhancing the color uniformity of WLEDs, improving scattering in phosphor layer is considered to be the most effective. In this paper, ZnO is used for that purpose. The results show that ZnO particle size significantly affects scattering in the phosphor layer, which is a vital factor to analyze scattering, scattering sand surface, scattering coefficient and scattered phase function  $C_{sca}(D, \lambda)$ ,  $\mu_{sca}(\lambda)$  and  $\rho(\theta, \lambda)$ . In addition, the concentration of ZnO was also analyzed with values from 2% to 22%. Color homogeneity depends not only on size but also on the concentration of added ZnO. Therefore, color homogeneity control is the control of ZnO size and concentration. The proposed result is 10% ZnO for the highest lumen of LED. With 14% and 500 nm of ZnO particles,  $\Delta CCT$  reaches the lowest. Depending on the production needs, manufacturers can choose the most appropriate way. However, with both required lumen and  $\Delta CCT$ , 14% ZnO is suitable for ZnO sizes.

Copyright © 2020 Institute of Advanced Engineering and Science.  
All rights reserved.

---

## Corresponding Author:

Nguyen Doan Quoc Anh,

Power System Optimization Research Group,

Faculty of Electrical and Electronics Engineering,

Ton Duc Thang University,

No. 19 Nguyen Huu Tho Street, Tan Phong Ward, District 7, Ho Chi Minh City, Vietnam.

Email: nguyendoanquocanh@tdtu.edu.vn

---

## 1. INTRODUCTION

With outstanding performance and remarkable features that improve the lighting efficiency, durability, power-saving as well as the low waste-emission rate, the Light-emitting diodes (LEDs) has grown passed many traditional lighting methods and become one of the most reliable light source for modern solid-state lighting [1-4]. However, to keep the development going, there must be improvements in the way that the white light in these LEDs is produced, which is integrating the blue light from a chip and yellow light from yellowish phosphor, known as YAG:Ce [5, 6]. Although this method is cost-effective regard of its lumen output, the chromatic quality is rather poor and often results in unwanted effect called “the yellow ring” that damaged the color output [7-9]. Intensive studies have been conducted on the issues and many productive solutions were proposed such as conformal configuration [10], rearrangement of phosphor material [11], focal point plan [12], and stacking configuration [13-16]. In spite of the fact that these strategies were affirmed to accomplish high CCT consistency, they additionally brought enormous creation challenges and staggering expense for the large scale manufacturing, which would constrain their applications in Drove bundling industry. In this manner, it is important to discover a strategy which acknowledges CCT consistency as well as is carried out with minimal effort and basic manufacture. To reply to this expectation, the diffuser restraint system which prioritize the focal point, simplicity, and effectiveness, that can improve the CCT consistency is a considerable option. In an attempt to achieve similar point, the oxide that are forms

between metals such as  $\text{TiO}_2$ ,  $\text{ZrO}_2$  and  $\text{SiO}_2$  have been utilized in several LED configuration to stabilize the CCT [17-21]. Chen and his partners applied  $\text{TiO}_2$  diffuser-loaded encapsulation to accomplish the enhancement in CCT uniformity as well as the reduction in CCT variance of remote phosphor white LEDs. Their research demonstrated the increases of angular color uniformity and luminous flux by 31.82% and 8.65%, respectively, when  $\text{TiO}_2$  diffuser is utilized. Another paper of Liang et al. considered  $\text{TiO}_2$  as a potential element to proposed UV/ $\text{TiO}_2$ , a treatment for hazardous organic pollutants, because it is a catalyst that can give a constant oxidant source to water without having to be replenished. Besides, the team of Geng and Xu has already practiced the application of  $\text{SiO}_2$  by forming the composition QDs- $\text{SiO}_2$ -BNAs and used it to create QDs- $\text{SiO}_2$ -BN nanoplate, which can eliminate thermal quenching, an effect induced by inadequate heat conduction and the high heat retaining limit in QDs- $\text{SiO}_2$  material, and improve the stability of QDs in LEDs. In addition to these aforementioned materials, researchers also interested in combining  $\text{CaF}_2$  with other phosphor patterns to enhance the performance of WLEDs, owing to the outstanding optical properties and high thermal conductivity of this particle. Bhanvase's team is one of those researchers, and in their 2018 paper, they exhibited the optical and structural properties of  $\text{CaF}_2:\text{Eu}^{3+}$  synthesized by using ultrasound assisted method. According to their researches, the new synthesized  $\text{CaF}_2:\text{Eu}^{3+}$  phosphor has excitation band that agrees with the excitation range of LED; moreover, the  $\text{Eu}^{3+}$  ions elements has the peak excitation at 394 nm and exhibits 591 nm and 612 nm emission bands. Thus, they concluded that this  $\text{CaF}_2:\text{Eu}^{3+}$  can be a good red emitting material. In 2019, continuing investigating the application of  $\text{CaF}_2$ , Xie and Wang and their partners proposed  $\text{CaF}_2$ -YAG:Ce phosphor ceramic, which includes yellow-emitting YAG:Ce particles mixed with a non-luminescent  $\text{CaF}_2$  ceramic matrix. The results from their study showed that  $\text{CaF}_2$ -YAG:Ce phosphor ceramic increase the optical performance of WLEDs, specifically, the increased luminous flux, CCT and CRI are 359.7 lm, 4021-7941 K and 70.1-82.7, respectively. The potential to boost the effectiveness of these nanoparticles is high as they are compact and flexible which open directions for alterations yet there are not many manuscripts on utilizing nanoparticles in a creative structure as most research concentrate on how WLEDs react to the particles [22-24]. In the meantime, because of the lack of concentrated speculations and complex specialized direction, choosing an optimal nanoparticles material to effectively enhance the CCT is quite confusing and repetitive, especially for manufacturers.

As the search continues, nanostructure containing ZnO came across as a preferable solution above considering how easy it is to operate, manufacture and monitor [25, 26]. The nanostructure containing ZnO with the refractive index of ( $n = 2.0$ ) can act as a slope refractive record layer between GaN and air with refractive indices respectively being ( $n = 2.5$ ) and ( $n = 1$ ), providing that other elements that follow such as thermal performance, duration, and antecedent focus are accounted for. The finding in recent research that prove the use of ZnO in enhancing the effective of light extraction process in LEDs devices through experiments integrating ZnO in specialized nanostructure has inspired many innovative applications. Yet many possibilities are still neglected for ZnO utilization in improving other lighting criteria with Drove bundling beside the light output, specifically the effects of different ZnO particles structure on light power and CCT consistency. With that being said, the focus of research should be moved to these area for new discovery of ZnO nanostructure potential to improve light energy and CCT. Hence, acknowledging the remaining issues, this paper will present the effect of ZnO on the performance of WLEDs based on an analysis of ZnO morphologies, which has not been done in any aforementioned studies. Particularly, the impacts of the particle size and concentration of ZnO are investigated and demonstrated through mathematic system and figures. The attain results will provide a basis for selecting suitable ZnO's parameters that serve the demands of improving lumen efficacy and color homogeneity of WLED. Through measurement of scattering events in the WLED, the effect of size and concentration of ZnO is clarified. Research results are valuable reference for the application of ZnO.

## 2. RESEARCH METHOD

### 2.1. Physical and optoelectronic characterization

From Figure 1(a), we can observe the physical model of WLED with ZnO traits that is used in all the experiments presented in this research. The schematic image of WLED cross-section in Figure 1(b) demonstrates how arrangement of the component inside the device. The constructing process of this WLED model is conducted in the following sequence: first, a blue chip with GaN traits which emits at 450 nm and has the appraised intensity of 1 W at a 350 mA current was put in the business lead-outline bundle. Then, a composition of YAG:Ce yellow phosphor (D half,  $13 \pm 2 \mu\text{m}$ ) and silicone glue is form in 12 minutes with a vacuum homogenizer running at 1360 rpm and 0.2 MPa (the weight proportion between the yellow phosphor and the silicone is 3:8). The composition is diffused on the surrounding of the blue chip and dried at  $120^\circ\text{C}$  for 3 hours to form a phosphor coating layer. A glass hemisphere is put above the compound to protect it from contamination and impact. The final step would be curing the ZnO

nanoparticles by blending vacuumed environment and degassed before inserting them into the phosphor structure. The final mixture should be left till dried in room temperature at approximately 25°C. The field emission scanning electron microscope (FE-SEM, Merlin) is the tool to draft the surface structure of ZnO. The UV-Vis spectrometer (UV-Vis, Agilent Cary 5000) is used for the calculation of the transmission efficiency in films with ZnO. The Electro-optical values in films and WLEDs with ZnO were achieved using a specialized system (Multi Spectrums T-950/930). The conducting process of measuring the mentioned value are carried out in the same condition which is in the air and under consistent thermal condition (25°C).

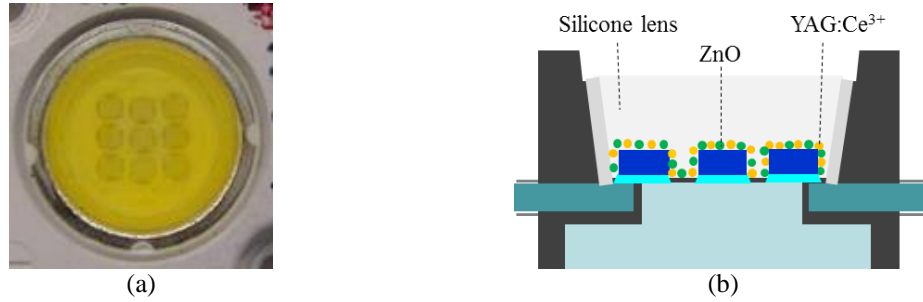


Figure 1. (a) Photograph of 9W WLED device and (b) schematic cross-sectional view of ZnO-doped WLED devices

## 2.2. Mie-scattering analysis

To calculate the scattered quantum-dot-converted elements (QDCEs), we can utilize the equation from Monte Carlo model [27] and apply the same way to measure the phosphor conversion in WLED. The equation below expressed the scattering coefficient and scattering phase function, which can be described as  $\mu_{sca}$  and  $\mu_{sca}(\lambda)$  respectively:

$$\mu_{sca} = \frac{c}{\bar{m}} \int f(D) C_{sca}(D, \lambda) dD \quad (1)$$

The scattering coefficient is the possibility that a scattering event occurs. The elements contribute to this value which presented above are  $c/\bar{m}$  for the thickness of QDs particles;  $c$  describes the QD concentration ( $\text{mg}/\text{cm}^3$ );  $D$  is the magnitude of particle in nm;  $\lambda$  is the measurement of wavelength in nm;  $f(D)$  is the distribution function of QD particle in size;  $\bar{m}$  depicts QD's mass (mg) in the QDCE, which can be calculated by integrating over  $f(D)$ ;  $C_{sca}(D, \lambda)$  is the QD's scattering cross-section, respectively, and can be calculated by:

$$C_{sca}(D, \lambda) = \frac{P_{sca}(D, \lambda)}{P_{inc}(\lambda)} = \frac{\int P_{sca}(D, \lambda) d\theta}{P_{inc}(\lambda)} \quad (2)$$

In which,  $P_{inc}(\lambda)$  is the source incident radiation ( $\text{W}/\text{m}^2$ );  $P_{sca}(D, \lambda)$  is the scattering energy (W), when light transmits through the QD;  $P_{sca}(\theta, D, \lambda)$  is the scattering power (W). The phase function of scattering that depicts the distribution of scattered energy meets the normalization conditions and can be observed in simplified form below:

$$\rho(\theta, \lambda) = \frac{\int f(D) \rho_{sca}(\theta, D, \lambda) / P_{sca}(D, \lambda) C_{sca}(D, \lambda) dD}{\int f(D) C_{sca}(D, \lambda) dD} \quad (3)$$

## 3. RESULTS AND ANALYSIS

To assess the effects of ZnO particles size on the scattering efficiency of WLED, we must consider different magnitude of ZnO particles with each distinct scattering feature. For example, the scattering cross-section of the ZnO particles,  $C_{sca}(D, \lambda)$  with the size varies from 400 nm, 500 nm to 600 nm, are shown in Figure 2(a-c). As the ZnO size increases,  $C_{sca}(D, \lambda)$  also increases, resulting in stronger scattering ability. Light tends to transmit straight to larger particles, which is beneficial to luminous flux. In contrast, light scatters in all directions with small particles. This is conducive to color uniformity but not

conductive to luminous flux. Dependent values  $C_{sca}(D, \lambda)$  and wavelength values  $C_{sca}(D, \lambda)$  decrease as the wavelength increases. Moreover, it is noticed that within the 380 nm wavelength, the maximum value  $C_{sca}(D, \lambda)$  can be achieved with all particle sizes. The scattering phase distributions are also measured responding to the size of ZnO particles of 400 nm, 500 nm, and 600 nm to determine the influences on scattering intensity.

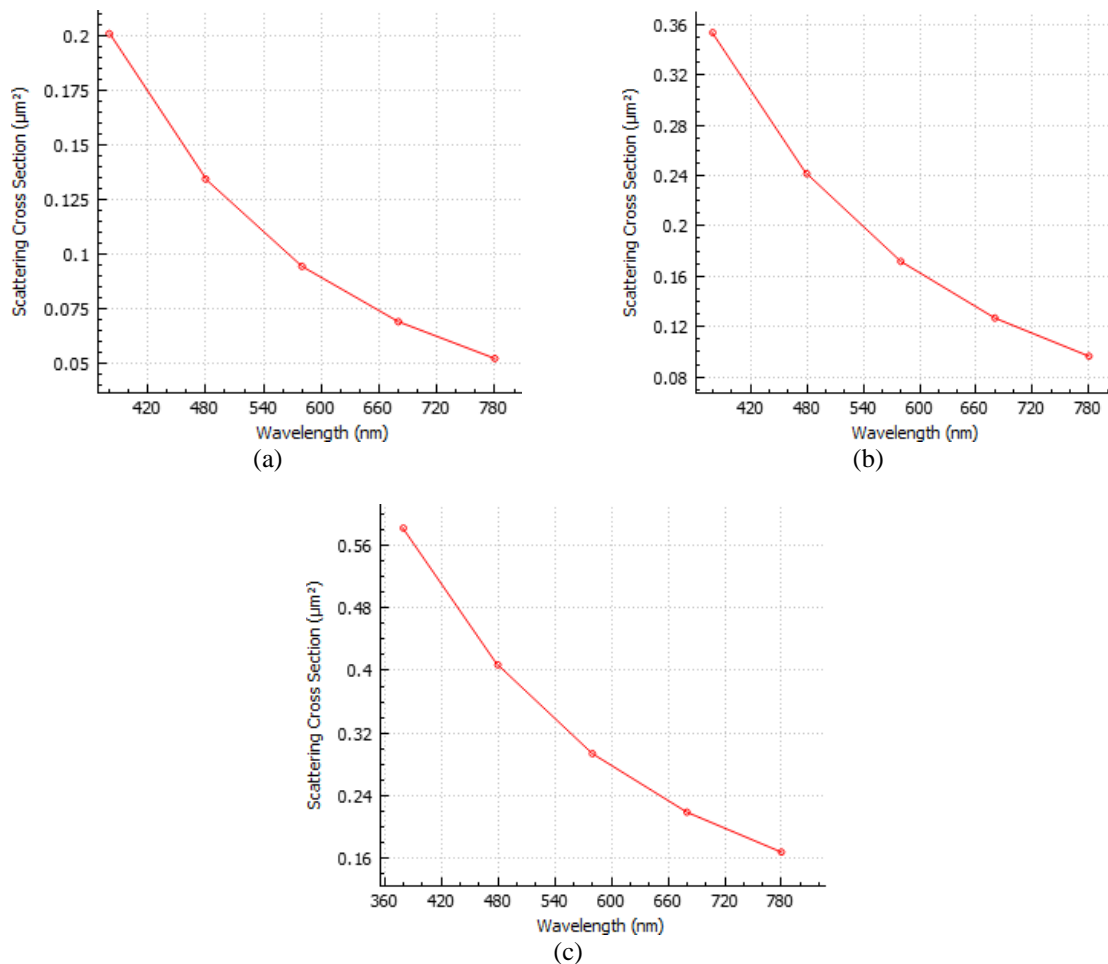


Figure 2. Scattering and cross-sections of ZnO particles with various sizes:  
(a) 400 nm, (b) 500 nm, (c) 600 nm

Similar to  $C_{sca}(D, \lambda)$ ,  $\mu_{sca}(\lambda)$  the value increases when the ZnO particle size increases. This further confirmed the scattering ability of ZnO particles increased. However, the larger the wavelength is, the smaller  $\mu_{sca}(\lambda)$  becomes. The maximum value is accomplished at 380 nm, which is suitable for the application of ZnO particles to improve light quality. It is possible to explain this phenomenon to  $C_{sca}(D, \lambda)$ ,  $\mu_{sca}(\lambda)$ , like this:

- We need to increase the scattering ability in the layers of phosphor so that the emitted light are mixed more times to make the white light emit color copper.
- Scattering value peaks at 380 nm, then gradually decreasing, and eventually reaching the smallest value at 780 nm. Meanwhile, the wavelength of the LED chip is 453 nm, which means that ZnO is suitable for advanced scattering in phosphor layers.

The results of Figure 2 confirm that the larger the ZnO particle size, the greater the scattering capacity. To determine which ZnO size is suitable for application,  $\rho(\theta, \lambda)$  should be considered.  $\rho(\theta, \lambda)$  shows the angle of scattering intensity, thus selecting suitable ZnO particle size depends on scattering and scattering ability. For large-sized particles, lights will be transmitted straight through them, leading to the benefited lumen. With a smaller particle size, the light is dispersed in many directions, meaning that

the scattering angle is large, and the energy of light is reduced by back scattering to the LED chip, resulting in lower lumen output. However, due to this multiple light scattering, blue and yellow rays are mixed more times before emitting from the phosphor layer to form white light.

Blue rays can be scattered more often with small ZnO particles. And these blue rays are sent to more LED chip sides. At this point, there is a combination of blue rays and "yellow ring" to form white light. The result are a reduction in the "yellow ring" effect and an improvement in color uniformity. The value  $\rho(\theta, \lambda)$  is clearly shown in Figure 3. The larger the ZnO particle size, the greater the intensity of scattering but the smaller the scattering angle. These findings clearly demonstrate the significant effects of ZnO particle sizes on two crucial optical properties of WLEDs, color uniformity and luminous flux. Thus, this helps manufacturers figure out the suitable size of ZnO particles when applied them in production.

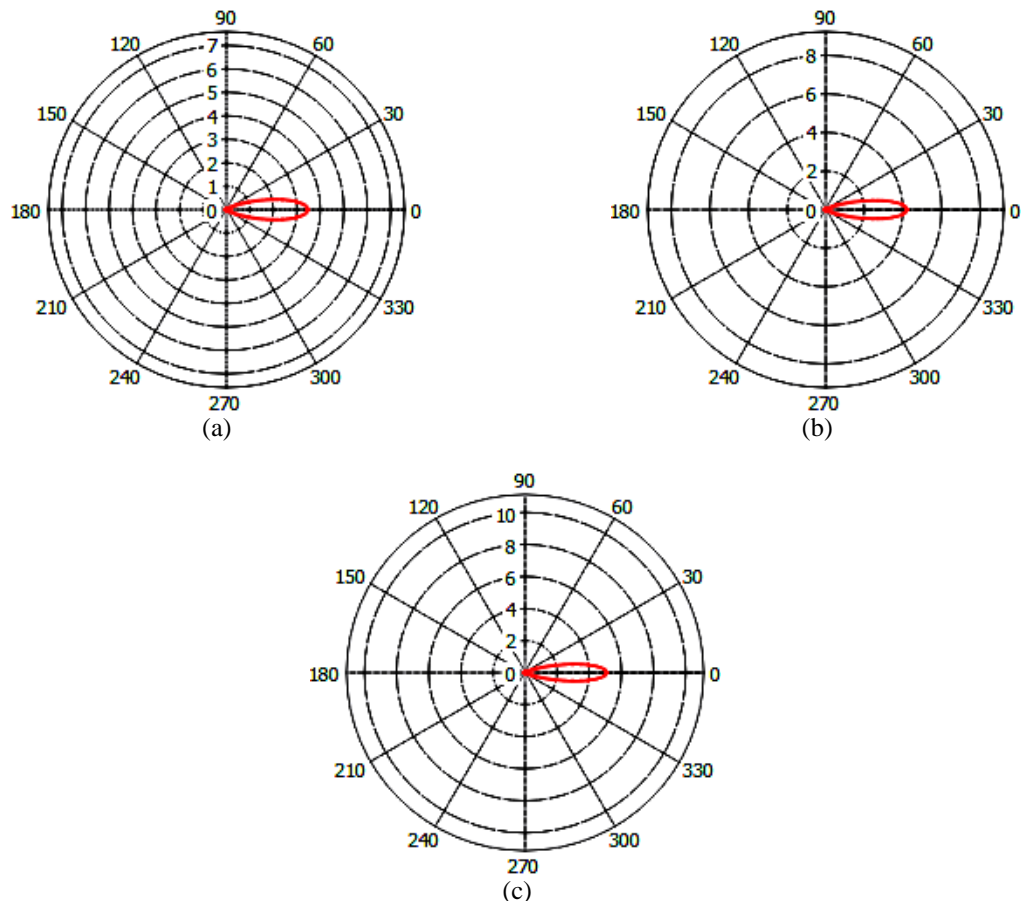


Figure 3. Scattering phase distributions of ZnO particles with various sizes:  
(a) 400 nm, (b) 500 nm, and (c) 600 nm

However, to investigate the lumen emitted, the size information is not enough. The emitted lumen is also influenced by the concentration of ZnO in the phosphor layer, as presented in Figure 4. As the concentration of ZnO increases, the passing lumen tends to decrease significantly at any size. As the ZnO concentration increases, the scattering capacity also increases, and the energy for this large scattering reduces the energy of light emitted. Therefore, choosing the right size and concentration of ZnO becomes very important in production. Based on the result of Figure 4, ZnO concentration of about 10% can be selected at any size to achieve the highest lumen. However, the goal of the study is not only the lumen emitted, but also the color uniformity, so we continue to consider the results in Figure 5 which depicts the reponse of  $\Delta CCT$  in WLED to different size and concentration of ZnO.

With 14% ZnO, though  $\Delta CCT$  does not reach the lowest level, it decreases significantly. Moreover,  $\Delta CCT$  has the lowest value with 500 nm ZnO at 14% concentration. In addition, it is easy to realize that  $\Delta CCT$  tends to decrease with the increasing concentration of ZnO. This can be explained by excessive scattering in the phosphor layer, from which the amount of scattered blue light becomes redundant, especially

with smaller size of ZnO particles. To achieve color uniformity, which means that  $\Delta CCT$  must be low, there must be a balance between the intensity of blue and yellow. Calibration of the size and ZnO concentration also aims at this. When the golden light prevailed, the "yellow ring" phenomenon appeared, the white light emitted was warm white light. At this time, the scattering of blue light is next feature to improve. Therefore, based on ZnO particle scattering survey through values  $C_{sca}(D, \lambda)$ ,  $\mu_{sca}(\lambda)$  and  $\rho(\theta, \lambda)$ , as well as the investigation in the concentration of ZnO, we can fully select the suitable ZnO particle parameters for application. If the manufacturer's request is a lumen emitted, 10% ZnO can be added to the phosphor layer regardless of particles' sizes. If the manufacturers aim to achieve the color uniformity, it is possible to choose 14% ZnO. And, if the manufacturer's goal is the enhancement in both lumen and color copper, 14% ZnO is the most suitable option.

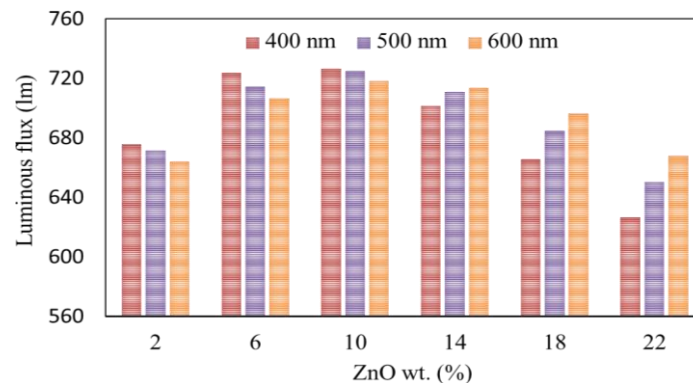


Figure 4. Lumen output of WLED as a function of the size and concentration of ZnO particles

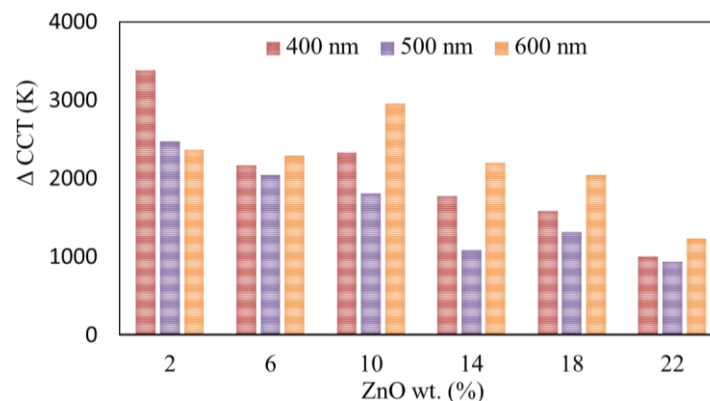


Figure 5.  $\Delta CCT$  of WLED as a function of the size and concentration of ZnO particles

#### 4. CONCLUSION

The paper successfully presents the effects of ZnO particles in two aspects of WLED, color uniformity and lumen output. In this study, we apply the mixture of ZnO and YAG:Ce in which the 400-600 nm ZnO were added to YAG:Ce to increase the scattering in phosphor layer. Increased scattering is an idea to improve color uniformity. However, it is necessary to select roofing to prevent excessive lumen emission. Through value  $C_{sca}(D, \lambda)$ ,  $\mu_{sca}(\lambda)$  and  $\rho(\theta, \lambda)$  analysis, the paper analyzed the scattering of ZnO particles by size clearly. Moreover, ZnO concentration is also mentioned so that producers have an overview of ZnO application. In other words, this article analyzed the two important factors of ZnO application which are the size and concentration through mathematic system and experiments. The proposed results show that lumen output of WLED can achieve the highest value with 10% ZnO. Meanwhile, with 14% concentration and 500 nm particle size of ZnO,  $\Delta CCT$  reaches the lowest level. Depending on the production needs, manufacturers can choose the most suitable concentration of ZnO. However, with both the required lumen and  $\Delta CCT$  required, 14% ZnO is suitable for applied ZnO sizes. With the useful information provided in this paper, we believe that manufacturer can improve their WLED products by selecting suitable ZnO particles' parameters.

## REFERENCES

- [1] S. K. Abeysekera, et al., "Impact of circadian tuning on the illuminance and color uniformity of a multichannel luminaire with spatially optimized LED placement," *Optics Express*, vol. 28, issue 1, pp. 130-145, 2020.
- [2] Q. W. Xu, et al., "Nanocrystal-filled polymer for improving angular color uniformity of phosphor-converted white LEDs," *Applied Optics*, vol. 58, issue 27, pp. 7649-7654, 2019.
- [3] R. E. Christiansen, et al., "Inverse design of nanoparticles for enhanced Raman scattering," *Optics Express*, vol. 28, issue 4, pp. 4444-4462, 2020.
- [4] Jiasheng, et al., "Color uniformity enhancement for COB WLEDs using a remote phosphor film with two freeform surfaces," *Optics Express*, vol. 24, issue 1, pp. 23685-23696, 2016.
- [5] Yongzhang, et al., "Luminescence of Tb<sup>3+</sup>/Eu<sup>3+</sup> codoped LiYF<sub>4</sub> single crystals under UV excitation for white-light LEDs," *Chinese Optics Letters*, vol. 13, issue 7, pp. 071601, 2015.
- [6] Xiangtian, et al., "Improving the modulation bandwidth of LED by CdSe/ZnS quantum dots for visible light communication," *Optics Express*, vol. 24, issue 19, pp. 21577-21586, 2016.
- [7] Yu, et al., "Phosphor-free Monolithic High-Efficiency White Light-Emitting-Diodes on Ternary InGaN Substrates," *CLEO: OSA Technical Digest*, pp. 1-2, 2015.
- [8] Yanru, et al., "Composite phase ceramic phosphor of Al<sub>2</sub>O<sub>3</sub>-Ce:YAG for high efficiency light emitting," *Optics Express*, vol. 23, issue 14, pp. 17923-17928, 2015.
- [9] Haibo, et al., "Cymbal-shaped phosphor structure for phosphor-converted white LEDs," *Optics Express*, vol. 23, no. 15, pp. A949-A956, 2015.
- [10] Yun, et al., "Energy transfer induced improvement of luminescent efficiency and thermal stability in phosphate phosphor," *Optics Express*, vol. 24, issue 4, pp. 4316-4330, 2016.
- [11] C. Fu, et al., "Raman determination of carrier concentration in ZnO-based heterostructure light-emitting diodes," *Optics Letters*, vol. 44, issue 7, pp. 1576-1579, 2019.
- [12] Y. J. Park, et al., "Development of high luminous efficacy red-emitting phosphor-in-glass for high-power LED lighting systems using our original low T<sub>g</sub> and T<sub>s</sub> glass," *Optics Letters*, vol. 44, issue 24, pp. 6057-6060, 2019.
- [13] Chiang, et al., "Effects of phosphor distribution and step-index remote configuration on the performance of white light-emitting diodes," *Optics Letters*, vol. 40, issue 12, pp. 2830-2833, 2015.
- [14] Michael, et al., "High luminous flux from single crystal phosphor-converted laser-based white lighting system," *Optics Express*, vol. 24, issue 2, pp. A215-A221, 2016.
- [15] Bin, et al., "Structural optimization for remote white light-emitting diodes with quantum dots and phosphor: packaging sequence matters," *Optics Express*, vol. 24, issue 26, pp. A1560-A1570, 2016.
- [16] Le, et al., "Highly efficient narrow-band green and red phosphors enabling wider color-gamut LED backlight for more brilliant displays," *Optics Express*, vol. 23, issue 22, pp. 28707-28717, 2015.
- [17] Shaojun, et al., "Energy transfer between Ce<sup>3+</sup> and Tb<sup>3+</sup> and the enhanced luminescence of a green phosphor SrB<sub>2</sub>O<sub>4</sub>:Ce<sup>3+</sup>, Tb<sup>3+</sup>, Na<sup>+</sup>," *Optical Materials Express*, vol. 6, issue 4, pp. 1172-1185, 2016.
- [18] Shudong, et al., "Angular color uniformity enhancement of white light-emitting diodes by remote micro-patterned phosphor film," *Photonics Research*, vol. 4, issue 4, pp. 140-145, 2016.
- [19] Huajuan, et al., "Close-relationship between the luminescence and structural characteristics in efficient nano-phosphor Y<sub>2</sub>Mo<sub>4</sub>O<sub>15</sub>:Eu<sup>3+</sup>," *Optical Materials Express*, vol. 5, issue 3, pp. 490-496, 2015.
- [20] Linlin, et al., "Near-infrared quantum cutting in Nd<sup>3+</sup> and Yb<sup>3+</sup> Doped BaGd<sub>2</sub>ZnO<sub>5</sub> phosphors," *Optical Materials Express*, vol. 5, issue 4, pp. 756-763, 2015.
- [21] Hirokazu, et al., "High energy-transfer rate from Sn<sup>2+</sup> to Mn<sup>2+</sup> in phosphate glasses," *Optical Materials Express*, vol. 5, issue 3, pp. 617-622, 2015.
- [22] Hiroyo, et al., "Europium-doped SiAlON and borosilicate glass composites for white light-emitting diode," *Applied Optics*, vol. 54, issue 29, pp. 8727-8730, 2015.
- [23] Dick, et al., "High-brightness source based on luminescent concentration," *Optics Express*, vol. 24, issue 14, pp. A1069-A1074, 2016.
- [24] Chen, et al., "Efficient hybrid white light-emitting diodes by organic-inorganic materials at different CCT from 3000K to 9000K," *Optics Express*, vol. 23, issue 7, pp. A204-A210, 2015.
- [25] S. -J. Kim, et al., "Enhanced performance of InGaN/GaN MQW LED with strain-relaxing Ga-doped ZnO transparent conducting layer," *Optics Express*, vol. 27, issue 8, pp. A458-A467, 2019.
- [26] Z. Huang, et al., "Investigation on the p-type formation mechanism of nitrogen ion implanted ZnO thin films induced by rapid thermal annealing," *Optical Materials Express*, vol. 9, issue 7, pp. 3098-3108, 2019.
- [27] J. X. Chen, et al., "Electroluminescence from light-emitting devices based on erbium-doped ZnO/n-Si heterostructures: Enhancement effect of fluorine co-doping," *Optics Express*, vol. 27, issue 21, pp. 30919-30930, 2019.